MNRAS **480,** L1–L5 (2018)
Advance Access publication 2018 June 06
doi:10.1093/mnrasl/sly102

Two planetary systems with transiting Earth-sized and super-Earth planets orbiting late-type dwarf stars

E. Díez Alonso,[1] J. I. González Hernández,[2,3] S. L. Suárez Gómez,[4] D. S. Aguado,[2] C. González Gutiérrez,[1] A. Suárez Mascareño,[5] A. Cabrera-Lavers,[2,6] J. González-Nuevo,[4] B. Toledo–Padrón,[2,3] J. Gracia,[7] F. J. de Cos Juez[1]★ and R. Rebolo[2,3,8]

[1]*Department of Exploitation and Exploration of Mines, University of Oviedo, E-33004 Oviedo, Spain*
[2]*Instituto de Astrofísica de Canarias, La Laguna, E-38205 Tenerife, Spain*
[3]*Universidad de La Laguna, Dpto. Astrofísica, La Laguna, E-38206 Tenerife, Spain*
[4]*Departamento de Física, Universidad de Oviedo, C. Federico García Lorca 18, E-33007 Oviedo, Spain*
[5]*Observatoire Astronomique de l' Université de Gèneve, CH-1290 Versoix, Switzerland*
[6]*GRANTECAN, Cuesta de San José s/n, Breña Baja, E-38712 La Palma, Spain*
[7]*Department of Construction and Manufacturing Engineering, University of Oviedo, E-33203 Oviedo, Spain*
[8]*Consejo Superior de Investigaciones Científicas, E-28006 Madrid, Spain*

Accepted 2018 June 4. Received 2018 May 25; in original form 2018 April 25

ABSTRACT

We present two new planetary systems found around cool dwarf stars with data from the K2 mission. The first system was found in K2-239 (EPIC 248545986), characterized in this work as M3.0V and observed in the 14th campaign of K2. It consists of three Earth-sized transiting planets with radii of 1.1, 1.0, and 1.1 $R_\oplus$, showing a compact configuration with orbital periods of 5.24, 7.78, and 10.1 d, close to 2:3:4 resonances. The second was found in K2-240 (EPIC 249801827), characterized in this work as M0.5V and observed in the 15th campaign. It consists of two transiting super-Earths with radii 2.0 and 1.8 $R_\oplus$ and orbital periods of 6.03 and 20.5 d. The equilibrium temperatures of the atmospheres of these planets are estimated to be in the range of 380–600 K and the amplitudes of signals in transmission spectroscopy are estimated at ∼10 ppm.

Key words: techniques: photometric – techniques: spectroscopic – planets and satellites: detection – stars: low mass – stars: individual: K2-239, K2-240.

1 INTRODUCTION

Low-mass stars are primary targets in the search for Earth-sized planets and in the study of their properties. Low-mass stars ($0.1\ M_\odot < M < 0.6\ M_\odot$) account for 70 per cent of the stellar population in the Milky Way (Henry, Kirkpatrick & Simons 1994), meaning they have a hugely significant impact in the overall statistics of planets in the Galaxy. Exoplanets with close-in orbits tend to be terrestrial when the mass of the star decreases (Howard et al. 2012), with an average of ∼0.5 Earth-sized rocky planet with $P_{\rm orb} < 50$ d around each low-mass star (Dressing & Charbonneau 2015).

Transiting Earth-sized planets induce deeper dimmings in the light curve of low mass stars and stronger radial velocity signals than in more massive stars. Temperate planets orbit closer and have shorter orbital periods, so it is easier to detect planets in the habitable zone (orbital range in which a planet's atmosphere can warm the surface to allow surface liquid water; Anglada-Escudé et al. 2016; Gillon et al. 2017). Signals in transit transmission spectroscopy (Charbonneau et al. 2002) are also stronger for stars with a small radius, so planets orbiting near bright low-mass stars are also suitable for atmospheric characterization (Kreidberg et al. 2014).

Detecting transiting planetary systems is of great value in terms of estimating the mass and density of their planets measuring transit timing variations (Gillon et al. 2017), which are stronger for compact systems in resonances. These systems are also suitable for testing the formation scenarios from the study of resonances that could be the result of migrations (Papaloizou & Szuszkiewicz 2005).

Until now, the Kepler mission (Borucki et al. 2010) has been the most successful facility detecting exoplanets by the transit method. Since the beginning of 2014, Kepler has been on its second mission (K2) (Howell et al. 2014), monitoring different fields near the ecliptic plane for ∼80 d. K2 has found many exoplanet candidates

★ E-mail: fjcos@uniovi.es (FJCJ); suarezsergio@uniovi.es (SLSG)

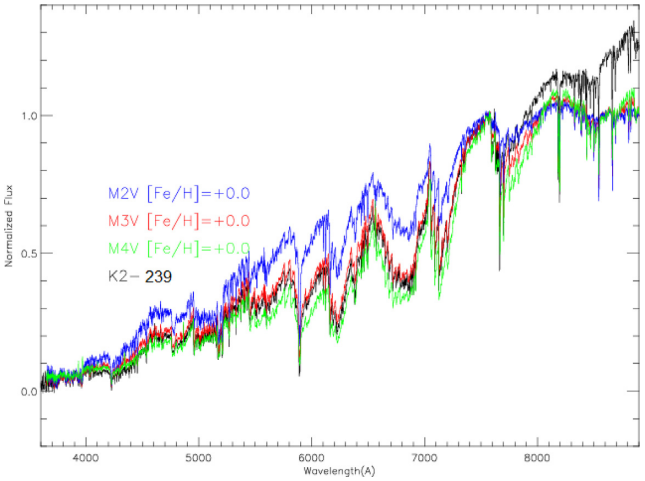

Figure 1. OSIRIS spectrum of K2-239 compared with reference spectra of M2.0V–M4.0V stars. Best fitting is obtained for M3V star with [Fe/H] ∼0. All spectra are normalized at $\lambda = 7575$ Å.

(Vanderburg et al. 2015; Crossfield et al. 2016; Díez Alonso et al. 2018; Hirano et al. 2018) in each observation campaign.

Campaign 14 was conducted between 2017 May 31 and 2017 August 19, centring on the Leo and Sextant area (central coordinates $\alpha = 10{:}42{:}44$, $\delta = +06{:}51{:}06$). Campaign 15 ran between 2017 August 23 and 2017 November 20, observing the area towards the constellation of Scorpius (central coordinates $\alpha = 15{:}34{:}28$, $\delta = -20{:}04{:}44$).

In this study we present the detection of two planetary systems during these campaigns. The first consists of three Earth-sized transiting planets orbiting K2-239 (EPIC 248545986; $\alpha = 10{:}42{:}22.633$, $\delta = +04{:}26{:}28.86$), observed in long cadence mode during campaign 14. The second consists of two transiting super-Earths orbiting K2-240 (EPIC 249801827; $\alpha = 15{:}11{:}23.907$, $\delta = -17{:}52{:}30.78$), observed in long cadence mode during campaign 15.

2 SPECTROSCOPIC AND PHOTOMETRIC DATA

2.1 Stellar characterization: K2-239

On 2018 March 13 we obtained spectra of K2-239 with the OSIRIS camera spectrograph (Cepa et al. 2000) of the 10.4 m Gran Telescopio Canarias (GTC), located at Observatorio Roque de los Muchachos in La Palma (Canary Islands, Spain). Three medium-resolution spectra ($\lambda/\delta\lambda \sim 2500$) in each of the *U, V, R, and I* bands were reduced in the standard manner, flux calibrated, telluric corrected, and finally combined into a single spectrum (see Fig. 1).

The spectrum was compared with SDSS/BOSS (Baryon Oscillation Spectroscopic Survey) reference spectra of M-type stars from Kesseli et al. (2017). The comparison was made with the HAMMER code (Covey et al. 2007), obtaining the best fit for an M3V star with [Fe/H] ∼0. The relative intensity of the NaI lines at 5890 and 8180 Å rule out the possibility of the star being giant, while the relative depth of the strong molecular bands of TiO at 7000–7300 Å points to [Fe/H] ∼ 0. Maldonado et al. (2015), working with measurements of spectral index from High Accuracy Radial velocity Planet Searcher spectra, conclude $T_{\rm eff} \sim 3450 \pm 50$ K for M3V stars, which is in agreement with our estimates of the stellar parameters.

Table 1. Stellar parameters for K2-239 and K2-240.

Parameter	K2-239	K2-240	Source
V (mag)	14.549 ± 0.040	13.392 ± 0.010	(1)
R (mag)	13.906 ± 0.020	12.804 ± 0.010	(1)
I (mag)	12.718 ± 0.030	11.994 ± 0.050	(1)
J (mag)	10.781 ± 0.026	10.394 ± 0.027	(2)
H (mag)	10.192 ± 0.021	9.745 ± 0.024	(2)
K (mag)	9.971 ± 0.021	9.560 ± 0.023	(2)
$T_{\rm eff}$ (K)	3420 ± 18	3810 ± 17	(3)
[Fe/H]	-0.1 ± 0.1	-0.1 ± 0.1	(3)
Radius ($R_\odot$)	0.36 ± 0.01	0.54 ± 0.01	(3)
Mass ($M_\odot$)	0.40 ± 0.01	0.58 ± 0.01	(3)
Luminosity ($L_\odot$)	0.016 ± 0.001	0.053 ± 0.002	(3)
$\log g$ (cgs)	4.9 ± 0.1	4.7 ± 0.1	(3)
$P_{\rm rot}$ (d)	–	10.8 ± 0.1	(3)
Distance (pc)	49 ± 3	70 ± 3	(3)
μ_α (mas yr^{-1})	-41.0 ± 3.9	-53.6 ± 1.5	(1)
μ_δ (mas yr^{-1})	10.5 ± 8.4	-49.8 ± 1.0	(1)
U, V, W (km s^{-1})	$-6.8, 4.2, -10.2$	$-5.4, -23.6, -1.7$	(3)

(1) UCAC4 (Zacharias et al. 2013).
(2) 2MASS (Cutri et al. 2003).
(3) This work.

Fig. 1 plots our comparison of the OSIRIS spectrum of K2-239 with reference spectra from M2.0V to M4.0V stars.

We computed the stellar parameters from J,H,V,K magnitudes listed in Table 1, applying the empirical relationships established by Mann et al. (2013, 2015) and Pecaut & Mamajek (2013), using the tabulated stellar parameters from Pecaut & Mamajek (2013) and the Mass–Luminosity relation for Main-sequence M dwarfs from Benedict et al. (2016). All the parameters are listed in Table 1.

Taking $m_V = 14.549 \pm 0.040$ (Table 1) and $M_V = 11.09 \pm 0.10$ from Pecaut & Mamajek (2013) tabulated parameters, we estimate a distance to K2-239 of 49 ± 3 pc.

We measured a radial velocity from the OSIRIS spectrum $v_{\rm r} = -8.5 \pm 1.5$ kms^{-1}, which combined with the estimated distance and the proper motions $\mu_\alpha = -41.0 \pm 3.9$ mas yr^{-1} and $\mu_\delta = 10.5 \pm 8.4$ mas yr^{-1}, results in the velocity components listed in Table 1. From the probability distributions of Reddy, Lambert & Allende Prieto (2006), we derive that K2-239 is a member of the Galactic thin disk.

2.2 Stellar characterization: K2-240

K2-240 has been observed by the Radial Velocity Experiment (RAVE; Steinmetz et al. 2006). RAVE's DR5 (Kunder et al. 2017) presents data from medium-resolution spectra ($R \sim 7500$) covering the Ca-triplet region (8410–8795 Å). From RAVE's DR5 we find for K2-240 (RAVE J151123.9-175231) $T_{\rm eff} = 3800 \pm 87$ K and $\log g = 4.50 \pm 0.17$, confirming that K2-240 is a cool dwarf star.

We repeated exactly the same analysis followed for K2-239 to derive the stellar parameters accurately, obtaining the parameters listed in Table1. These parameters are consistent with K2-240 being an M0.5V star.

We also note that a very clear rotation signal is present in the light curve from K2. From a Lomb-Scargle (Scargle 1982) analysis we estimate $P_{\rm rot} = 10.8 \pm 0.1$ d.

From RAVE's radial velocity $v_{\rm r} = 0.20 \pm 1.56$ km s^{-1}, our estimated distance of $d = 70 \pm 3$ pc, and proper motions $\mu_\alpha = -53.6 \pm 1.5$ mas yr^{-1} and $\mu_\delta = -49.8 \pm 1.0$ mas yr^{-1}, we com-

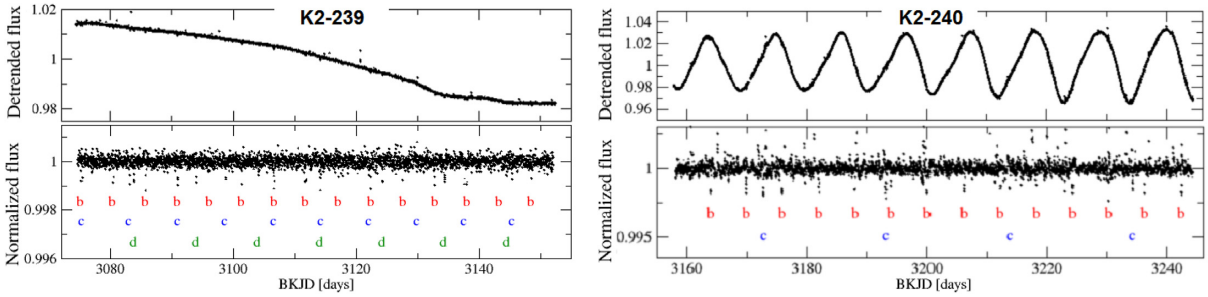

Figure 2. K2 detrended (top) and normalized (bottom) light curves for K2-239 (left) and K2-240 (right). Characters b, c, and d show times of observed transits for planets in each system.

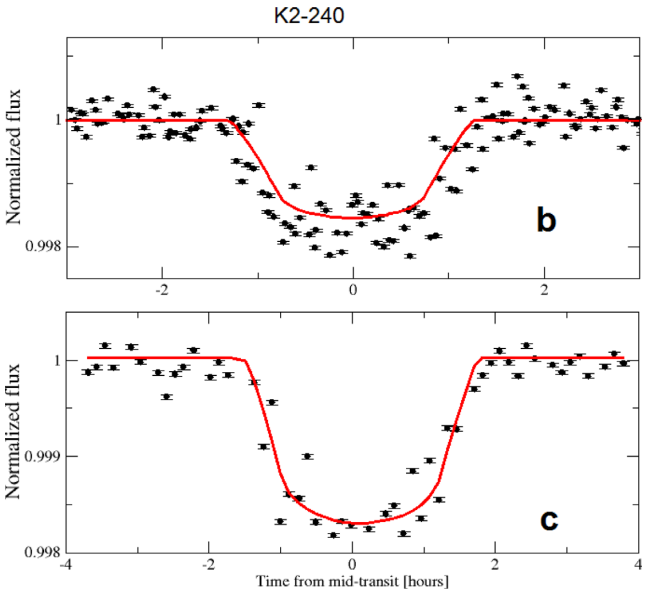

Figure 3. Phase-folded light curves corresponding to planets b (top), c (middle), and d (bottom) in the K2-239 system. Solid curves represent best model fits obtained by MCMC.

pute velocity components listed in Table 1. From the probability distributions of Reddy et al. (2006), we derive that K2-240 is a member of the Galactic thin disk.

2.3 K2 photometric data

We followed the work of Vanderburg & Johnson (2014) to analyse the K2-corrected photometry of our target stars, detrending stellar variability with a spline fit and searching for periodic signals using the Box Least Squares method (Kovács, Zucker & Mazeh 2002) on attained data. This analysis shows three transit signals with periods 5.240 ± 0.001 (b), 7.775 ± 0.001 (c), and 10.115 ± 0.001 d in K2-239 and two transit signals with periods 6.034 ± 0.001 (b) and 20.523 ± 0.001 (c) days in K2-240 (Fig. 2).

We performed Monte Carlo Markov Chain (MCMC) analysis on each phase-folded transit (Figs 3 and 4) to estimate the planetary parameters, fitting models from Mandel & Agol (2002) with the EXOFAST package (Eastman, Gaudi & Agol 2013). For each data point, the light curve was resampled 10 times uniformly spaced over the 29.5-min long cadence of K2 and averaged, following Kipping (2010). For the calculations, we set the values of $T_{\rm eff}$, log g, and [Fe/H] listed in Table 1, and orbital periods listed above.

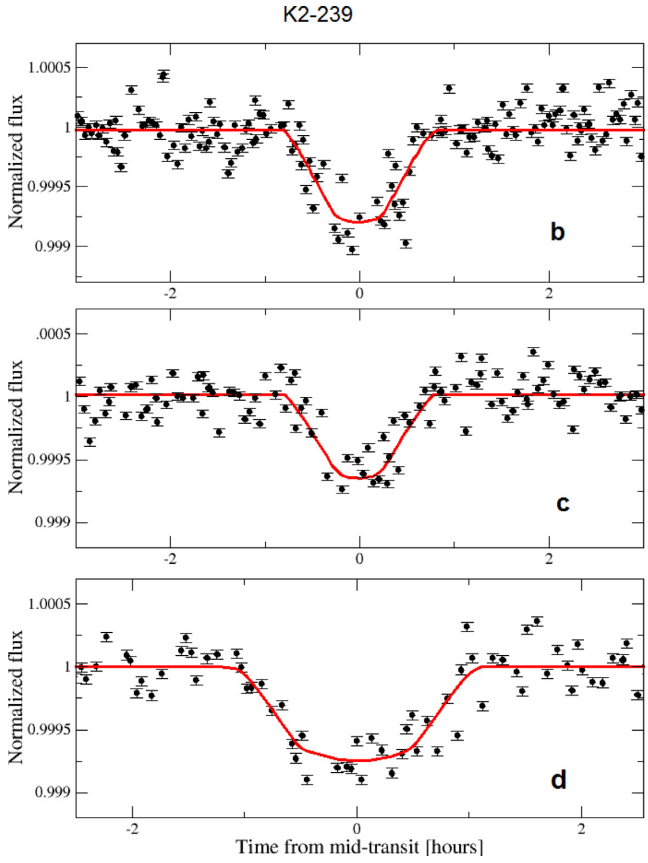

Figure 4. Phase-folded light curves corresponding to planets b (top) and c (bottom) in the K2-240 system. Solid curves represent best model fits obtained by MCMC.

We also worked with the assumption of eccentricity $e = 0$, valid for transiting planets in a multiplanetary system (Van Eylen & Albrecht 2015).

The planets in the K2-239 system have estimated radii of 1.1 ± 0.1 $R_\oplus$ (b), 1.0 ± 0.1 $R_\oplus$ (c), and 1.1 ± 0.1 $R_\oplus$ (d), orbital periods of 5.242 ± 0.001 d (b), 7.775 ± 0.001 d (c), and 10.115 ± 0.001 d (d), and semimajor axis of 0.0441 ± 0.0008 AU (b), 0.0576 ± 0.0009 AU (c), and 0.0685 ± 0.0012 AU (d).

The planets in the K2-240 system have estimated radii of $2.0^{+0.2}_{-0.1}$ $R_\oplus$ (b) and $1.8^{+0.3}_{-0.1}$ $R_\oplus$ (c), orbital periods of 6.034 ± 0.001 d (b) and 20.523 ± 0.001 d (c), and semimajor axis of 0.0513 ± 0.0009 AU (b), 0.1159 ± 0.0020 AU (c). Table 2 summarizes all the parameters obtained for the planets.

Table 2. Parameters for planets in the K2-239 and K2-240 systems.

Planet parameters	K2-239 b	K2-239 c	K2-239 d	K2-240 b	K2-240 c
Orbital period (P) (d)	5.240 ± 0.001	7.775 ± 0.001	10.115 ± 0.001	6.034 ± 0.001	20.523 ± 0.001
Semimajor axis (a) (AU)	0.0441 ± 0.0008	0.0576 ± 0.0009	0.0685 ± 0.0012	0.0513 ± 0.0009	0.1159 ± 0.0020
Radius (R_p) ($R_\oplus$)	1.1 ± 0.1	1.0 ± 0.1	1.1 ± 0.1	$2.0^{+0.2}_{-0.1}$	$1.8^{+0.3}_{-0.1}$
Mass (M_p) ($M_\oplus$)	1.4 ± 0.4	0.9 ± 0.3	1.3 ± 0.4	$5.0^{+0.5}_{-0.2}$	$4.6^{+0.7}_{-0.3}$
Equilibrium temperature (T_{eq}) (K)	502^{+22}_{-18}	427^{+24}_{-19}	399^{+18}_{-15}	586^{+24}_{-18}	389^{+19}_{-17}
Transit parameters	K2-239 b	K2-239 c	K2-239 d	K2-240 b	K2-240 c
Epoch (BKJD) (d)	3075.191	3083.860	3075.381	3163.825	3172.722
Radius of planet in stellar radii (R_p/R_*)	$0.0259^{+0.0013}_{-0.0012}$	$0.0241^{+0.0016}_{-0.0014}$	0.0255 ± 0.0012	0.0362 ± 0.0014	0.0313 ± 0.0024
Semimajor axis in stellar radii (a/R_*)	$24.6^{+1.9}_{-2.0}$	$34.0^{+3.3}_{-3.5}$	$38.8^{+2.9}_{-3.3}$	$21.1^{+1.3}_{-1.6}$	48.0 ± 4.4
Linear limb-darkening coeff (u_1)	$0.344^{+0.058}_{-0.055}$	$0.344^{+0.049}_{-0.050}$	0.345 ± 0.056	$0.402^{+0.068}_{-0.067}$	$0.411^{+0.071}_{-0.067}$
Quadratic limb-darkening coeff (u_2)	0.373 ± 0.053	$0.374^{+0.051}_{-0.050}$	$0.371^{+0.051}_{-0.052}$	$0.308^{+0.062}_{-0.063}$	$0.312^{+0.061}_{-0.064}$
Inclination (i) (deg)	$88.99^{+0.68}_{-0.87}$	$88.77^{+0.70}_{-0.57}$	$89.43^{+0.38}_{-0.45}$	$89.26^{+0.51}_{-0.64}$	$89.66^{+0.22}_{-0.26}$
Impact parameter (b)	$0.44^{+0.33}_{-0.29}$	$0.73^{+0.24}_{-0.39}$	0.39 ± 0.25	$0.28^{+0.20}_{-0.19}$	$0.29^{+0.18}_{-0.19}$
Transit depth (δ)	$0.00067^{+0.00007}_{-0.00006}$	$0.00058^{+0.00008}_{-0.00006}$	0.00065 ± 0.00006	0.00131 ± 0.00010	$0.00098^{+0.00016}_{-0.00015}$
Total duration (T_{14}) (d)	$0.0611^{+0.0067}_{-0.013}$	$0.052^{+0.013}_{-0.027}$	$0.0766^{+0.0058}_{-0.0073}$	$0.0897^{+0.0046}_{-0.0038}$	$0.133^{+0.011}_{-0.010}$

2.4 False positives analysis

We acquired images of K2-239 with the OSIRIS camera spectrograph on 2018 March 13. Night conditions were rather good, and data were collected under photometric conditions, a dark moon, and with an average seeing of 0.7 arcsec. For broad-band imaging, a series of 10 x 1 sec in Sloan *i* filter was obtained. Bias correction, flat fielding, and bad pixel masking were done using standard procedures, and the images were finally aligned (see Fig. 5, top panel). Analyses of final image exclude companions at 0.6 arcsec with $\delta_{mag} < 5.0$ and at 3 arcsec with $\delta_{mag} < 10$.

In the same way, images from POSS-I (Minkowski & Abell 1963) (year 1953) and 2MASS (Cutri et al. 2003) (year 1998, see Fig. 5, top panel) do not show background sources at the current star position.

At ExoFOP–K2[1] an AO image of K2-240 is available, acquired with the NIRC2 instrument at the 10 m Keck 2 telescope (Maunakea, Hawaii). The image excludes companions at 0.2 arcsec with $\delta_{mag} < 5.0$ and at 1 arcsec with $\delta_{mag} < 8.3$ (Fig 5, bottom panel).

Non-detection of blended objects in these images and the extremely low probability of multiple false positives as shown by Lissauer et al. (2011) confirm the planetary origin of transit signals in K2-239 and K2-240.

3 DISCUSSION AND CONCLUSIONS

Assuming the planet radii listed in Table 2, and the mean density for planets satisfying $R_p \leq 1.5R_\oplus$ from Weiss & Marcy (2014), we obtain $M_b = 1.4 \pm 0.4$ $M_\oplus$, $M_c = 0.9 \pm 0.3$ $M_\oplus$, $M_d = 1.3 \pm 0.4$ $M_\oplus$ for planets b, c, and d, respectively in the K2-239 system. Adopting $M_p \ll M_*$, circular orbits and $\sin i \sim 1$, we computed induced semi-amplitudes in stellar velocity variations of 0.9 ms^{-1} for planet b, 0.5 ms^{-1} for planet c, and 0.7 ms^{-1} for planet d, well-suited for radial velocity monitoring with ultrastable spectrographs such as ESPRESSO (Echelle SPectrograph for Rocky Exoplanets and Stable Spectroscopic Observations; Pepe et al. 2014; González Hernández et al. 2017) at the VLT.

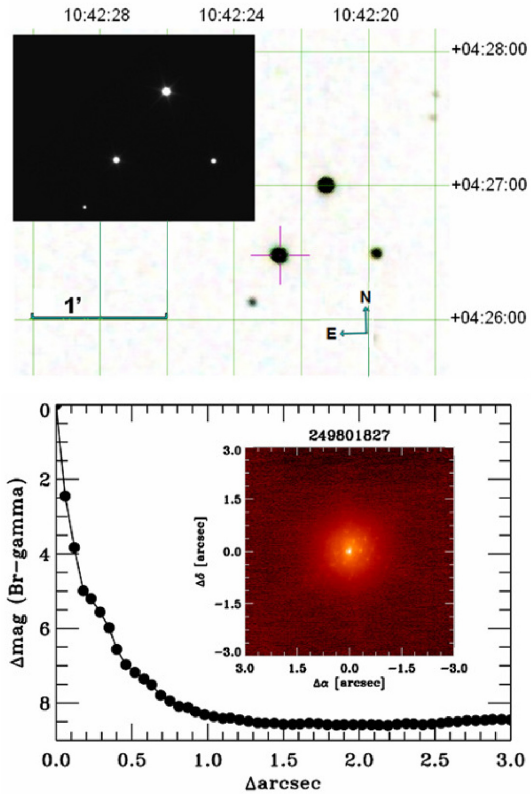

Figure 5. Top panel: OSIRIS/GTC image of K2-239 field taken with seeing 0.6 arcsec in the *i*-band Sloan filter, superimposed on the 2MASS image of the field. Bottom panel: contrast curve and AO image of K2-240 acquired with the NIRC2 instrument at the 10 m Keck-2 telescope.

[1] https://exofop.ipac.caltech.edu/k2/

The amplitude of the signal in transit transmission spectroscopy can be estimated as $\frac{R_p \cdot h_{\rm eff}}{(R_*)^2}$ (Gillon et al. 2016) with $h_{\rm eff}$ the effective atmospheric height. $h_{\rm eff}$ is related to the atmospheric scale height $H = K{\cdot}T/\mu \cdot g$ (K Boltzmann's constant, T atmospheric temperature, μ atmospheric mean molecular mass, and g surface gravity). Assuming $h_{\rm eff} = 7{\cdot}$H (Miller-Ricci & Fortney 2010) for a transparent volatile dominated atmosphere ($\mu = 20$) with 0.3 Bond albedo, we found amplitudes in transit transmission spectroscopy of 1.2×10^{-5} (b), 1.1×10^{-5} (c), and 10^{-5} (d).

We used the MERCURY package (Chambers 1999) to simulate and test the evolution and stability of the system for 10^6 yr. We simulated using Bulirsch–Stoer integrator, adopting circular orbits and masses from the mass–radius relation. We do not find significant changes in the eccentricity or in the inclination of the orbits, showing a dynamically stable system.

To estimate the masses for the planets of the K2-240 system, we used the mass–radius relation from Weiss & Marcy (2014) for planets satisfying $1.5 \leq R_{\rm p}/R_\oplus \leq 4$, obtaining $M_{\rm b} = 5.0^{+0.5}_{-0.2}$ M$_\oplus$, $M_{\rm c} = 4.6^{+0.7}_{-0.3}$ M$_\oplus$. Under the assumption of $M_{\rm p} \ll M_*$, circular orbits and $\sin i \sim 1$, we computed induced semi-amplitudes in stellar velocity variations of 2.5 ms^{-1} for planet b and 1.5 ms^{-1} for planet c. With the same assumptions as in the previous section, we estimate amplitudes in transit transmission spectroscopy of 1.2×10^{-5} (b) and 6.6×10^{-6} (c).

We also tested the stability of K2-240 system with the MERCURY package as described in the previous section. Again our simulations point towards a dynamically stable system.

The planetary systems presented in this work, with equilibrium temperatures estimated in the range of 380–600 K, are suitable targets for incoming facilities; Plato, monitoring in shorter cadence mode, could reveal transit timing variations that allow accurate planetary masses to be estimated. The James Webb Telescope could find signs of planetary atmospheres. Ultrastable spectrographs such as ESPRESSO at VLT, could also carry out radial velocity follow-up, so these are promising targets to improve our understanding of compact Earth-sized planetary systems (K2-239) and super-Earth systems on the rocky–gaseous boundary (EPIC K2-240).

ACKNOWLEDGEMENTS

EDA, CGG and JCJ acknowledge Spanish ministry project AYA2017-89121-P. JIGH, BTP, DSA, and RRL acknowledge the Spanish ministry project MINECO AYA2014-56359-P. JIGH also acknowledges financial support from the Spanish Ministry of Economy and Competitiveness (MINECO) under the 2013 Ramón y Cajal program MINECO RYC-2013-14875. ASM acknowledges financial support from the Swiss National Science Foundation (SNSF). JGN and SLSG acknowledge financial support from the I+D 2015 project AYA2015-65887-P (MINECO/FEDER). JGN also acknowledges financial support from the Spanish MINECO for a Ramón y Cajal fellowship (RYC-2013-13256).

Based on observations made with the Gran Telescopio Canarias (GTC), installed in the Spanish Observatorio del Roque de los Muchachos of the Instituto de Astrofísica de Canarias, in the island of La Palma.

REFERENCES

Anglada-Escudé G. et al., 2016, Nature, 536, 437
Benedict G. F. et al., 2016, AJ, 152, 141
Borucki W. J. et al., 2010, Science, 327, 977
Cepa J. et al., 2000, in Iye, M., Moorwood, A.F. eds, OSIRIS tunable imager and spectrograph, Proc. SPIE Vol. 4008, Munich, Germany, p. 623
Chambers J. E., 1999, MNRAS, 304, 793
Charbonneau D., Brown T. M., Noyes R. W., Gilliland R. L., 2002, ApJ, 568, 377
Covey K. R. et al., 2007, AJ, 134, 2398
Crossfield I. J. M. et al., 2016, ApJS, 226, 7
Cutri R. M., Skrutskie M. F., van Dyk S. et al., 2003.
Díez Alonso E. et al., 2018, MNRAS, 476, L50
Dressing C. D., Charbonneau D., 2015, ApJ, 807, 45
Eastman J., Gaudi B. S., Agol E., 2013, PASP, 125, 83
Gillon M. et al., 2016, Nature, 533, 221
Gillon M. et al., 2017, Nature, 542, 456
González Hernández J. I., Pepe F., Molaro P., Santos N., 2017, preprint (arXiv:1711.05250)
Henry T. J., Kirkpatrick J. D., Simons D. A., 1994, AJ, 108, 1437
Hirano T. et al., 2018, AJ, 155, 124
Howard A. W. et al., 2012, ApJS, 201, 15
Howell S. B. et al., 2014, PASP, 126, 398
Kesseli A. Y., West A. A., Veyette M., Harrison B., Feldman D., Bochanski J. J., 2017, ApJS, 230, 16
Kipping D. M., 2010, MNRAS, 408, 1758
Kovács G., Zucker S., Mazeh T., 2002, A&A, 391, 369
Kreidberg L. et al., 2014, Nature, 505, 69
Kunder A. et al., 2017, AJ, 153, 75
Lissauer J. J. et al., 2011, ApJS, 197, 8
Maldonado J. et al., 2015, A&A, 577, A132
Mandel K., Agol E., 2002, ApJ, 580, L171
Mann A. W., Brewer J. M., Gaidos E., Lépine S., Hilton E. J., 2013, AJ, 145, 52
Mann A. W., Feiden G. A., Gaidos E., Boyajian T., von Braun K., 2015, ApJ, 804, 64
Miller-Ricci E., Fortney J. J., 2010, ApJ, 716, L7
Minkowski R. L., Abell G. O., 1963, in Strand, K. A., ed. Basic Astronomical Data: Stars and Stellar Systems, Chicago Univ. Press, Chicago, IL USA, 481
Papaloizou J. C. B., Szuszkiewicz E., 2005, MNRAS, 363, 153
Pecaut M. J., Mamajek E. E., 2013, ApJS, 208, 9
Pepe F. et al., 2014, Astron. Nachr., 335, 8
Reddy B. E., Lambert D. L., Allende Prieto C., 2006, MNRAS, 367, 1329
Scargle J. D., 1982, ApJ, 263, 835
Steinmetz M. et al., 2006, AJ, 132, 1645
Van Eylen V., Albrecht S., 2015, ApJ, 808, 126
Vanderburg A., Johnson J. A., 2014, PASP, 126, 948
Vanderburg A. et al., 2015, ApJ, 800, 59
Weiss L. M., Marcy G. W., 2014, ApJ, 783, L6
Zacharias N., Finch C. T., Girard T. M., Henden A., Bartlett J. L., Monet D. G., Zacharias M. I., 2013, AJ, 145, 44

This paper has been typeset from a TEX/LATEX file prepared by the author.